

Does Resolution Matter? Satellite Imagery Comparison for Dynamic Fuel Mapping and Wildfire Risk Assessment

Nasimeh Rashidi, Washington State University, nasimeh.rashidi@wsu.edu

Ji Yun Lee, Washington State University, jiyun.lee@wsu.edu

Keywords: Satellite Imagery, Fuel Mapping, Wildfire Risk Assessment, Computer Vision, Machine Learning, Fuel Type Classification, Resolution Sensitivity

Abstract

In recent years, the increasing frequency and severity of wildfire have caused widespread devastation to infrastructure, communities, and ecosystems. Effective wildfire risk mitigation strategies require accurate and up-to-date information about the spatiotemporal distribution of vegetation, which serves as the primary fuel for wildfires. However, current approaches to fuel mapping typically rely on static datasets like LANDFIRE, which often lack the spatial precision and temporal relevance needed for accurate wildfire risk assessment. This study, therefore, presents an application-driven evaluation of a dynamic fuel mapping generation model using satellite imagery. Specifically, a K-nearest neighbors (KNN) algorithm is adapted and evaluated for pixel-wise fuel mapping, incorporating enhancements such as active learning and systematic sampling to improve classification robustness. Model performance is assessed across three sources of satellite imagery with different spatial resolutions: Harmonized Landsat and Sentinel-2 (HLS), Sentinel-2, and SPOT-6. Results show that classification success depends not only on resolution but also on the compatibility between input data and ground truth labels. Moreover, findings indicate that different satellite imagery resolutions are better suited for different mapping objectives, with high-resolution imagery offering advantages for fine-scale analysis, while lower-resolution data remain effective for regional assessments, highlighting the need for evaluation metrics and modeling approaches that account for both pixel-level accuracy and broader spatial patterns. This work contributes a scalable, interpretable, and dynamic fuel type classification approach and offers practical insights for sensor selection and data preparation in dynamic fuel mapping.

1. Introduction

In recent decades, wildfire activity has intensified across the western United States and other fire-prone regions, driven by rising temperatures, prolonged droughts, and changing land use patterns [1]. These changes not only increase the frequency and severity of wildfires but also alter vegetation recovery and succession dynamics [2], [3]. Vegetation type and structure, as the critical inputs for fire behavior models, influence ignition probability, fire spread, and intensity [4], [5]. Accurate and up-to-date fuel mapping, therefore, plays a foundational role in wildfire risk assessment, mitigation planning, and resource allocation.

However, most operational fuel datasets remain static, are updated infrequently, and often fail to capture rapid vegetation changes due to disturbances, seasonal cycles, or human interventions [6], [7], [8]. For instance, the LANDFIRE program, one of the most widely used national fuel data products in the United States, offers a valuable baseline but is typically updated on a multi-year cycle, making it insufficient for near-real-time fuel mapping and wildfire risk assessment [6], [7].

Moreover, these static maps may overlook subtle but important changes in fuel loads, especially in areas affected by rapid vegetation growth or decline following weather shifts or prescribed burns [9].

This study investigates the potential of satellite imagery with different spatial resolutions for dynamic fuel mapping, focusing on how varying levels of image detail impact classification accuracy, spatial coherence, and practical usability of fuel mapping. By comparing multiple distinct satellite imagery sources, we aim to explore their effectiveness in capturing critical features of the landscape, such as fuel type and distribution. Specifically, this study extracts spectral and statistical features from these images and leverages the K-Nearest Neighbors (KNN) for classification and analysis. Unlike deep learning models that often require extensive training datasets, complex model architectures, and substantial computational resources, KNN offers simplicity, adaptability, and ease of integration into operational workflows.

Several recent studies have highlighted the promise of remote sensing combined with machine learning (ML) for land cover and fuel type classification [10], [11], [12]. However, few have systematically examined how input resolution influences classification outcomes and model usability in dynamic wildfire contexts. This gap is addressed in our work through a comparative evaluation of classification performance across satellite sensors, focusing on how spatial resolution influences fuel mapping accuracy and reliability.

2. Methodology

This study employs a KNN classifier to dynamically map vegetative fuels at multiple spatial resolutions using satellite imagery. The datasets analyzed include Harmonized Landsat and Sentinel-2 (HLS) imagery with a 30-meter spatial resolution, Sentinel-2 imagery with a 10-meter resolution, and SPOT-6 with 6-meter resolution. HLS and Sentinel-2 are freely available and offer frequent revisit times, approximately every 2–3 days for HLS [13], and every 5 days for Sentinel-2 [14], making them suitable for dynamic fuel mapping applications. In contrast, SPOT-6 provides higher spatial resolution imagery, with a revisit time of approximately one day when operated jointly with SPOT-7, and between one and three days when operating independently [15]. However, SPOT imagery is commercially licensed and incurs significant costs, making it less suitable for routine or large-scale monitoring compared to freely available datasets. These trade-offs between spatial resolution, revisit frequency, and data accessibility are critical considerations when selecting appropriate datasets for dynamic fuel mapping and wildfire risk applications.

2.1. Data Preprocessing & Feature Extraction

For HLS and Sentinel-2, three temporal observations spanning the growing season were used to construct 18-band image stacks, with each time point contributing six spectral bands: red, green, blue, near-infrared (NIR), shortwave infrared 1 (SWIR1), and shortwave infrared 2 (SWIR2). For each of these 18 bands, five additional features (i.e., mean, standard deviation, skewness, kurtosis, and frequency content) were computed, resulting in a total of 48 features per pixel. Band values were normalized to ensure consistency across datasets, and native spatial resolutions, 30 meters for HLS and 10 meters for Sentinel-2, were retained. Preprocessed HLS and Sentinel-2 images were stored as 224×224 pixel patches. SPOT-6 imagery, with a spatial resolution of 6 meters, was processed separately due to its single-date, four-band structure consisting of red, green, blue, and NIR bands. To compensate for the lack of temporal depth, 17 additional features were extracted.

These included vegetation and moisture indices, such as the Normalized Difference Vegetation Index (NDVI), the Normalized Difference Water Index (NDWI), brightness, the Enhanced Vegetation Index (EVI), and the Visible Atmospherically Resistant Index (VARI). Local spatial information was incorporated by computing 3×3 neighborhood means and standard deviations for each band. Texture descriptors based on the Gray Level Co-occurrence Matrix (GLCM), including contrast, correlation, energy, and homogeneity, were also calculated. In total, 21 features per pixel were generated, and full spatial resolution was preserved. SPOT-6 data were handled as 56×56 pixel patches. For all three datasets, ground truth labels were derived from the LANDFIRE data distribution site using classifications based on the Scott and Burgan 40 standard fuel models. The LANDFIRE data have a spatial resolution of 30 meters, which can introduce limitations when used as ground truth for higher-resolution imagery such as Sentinel-2 and SPOT-6. In addition, due to potential outdated classification and inherent noise, the LANDFIRE data may not reliably align with the timing, spatial detail, or conditions captured in the satellite imagery used in this study. These limitations, along with their impacts on model performance, will be further discussed in Section 3. The main fuel categories used in this study included non-burnable (NB), grass (GR), grass–shrub mixture (GS), shrub (SH), timber understory (TU), and timber litter (TL). The slash/brown (SB) category was excluded from analysis due to its rarity in the United States. This category represents specific conditions, such as post-logging debris or blowdowns, and lacked a sufficient number of pixels available to reliably represent this fuel type. Ground truth masks were spatially aligned with the corresponding image patches and were used throughout the training, validation, and testing phases.

2.2. Classification Using KNN

A KNN classifier was applied to all three datasets to perform fuel type classification. Other machine learning models, such as decision trees (DT) and random forests (RF), were initially evaluated in a separate, related study [16], but they were found to be less effective for distinguishing the complex fuel categories. KNN was selected for this study due to its non-parametric structure and its strong performance in pixel-level classification tasks. Its ability to capture complex, non-linear relationships without relying on strict assumptions about data distribution made it particularly suitable for the spectral variability present in satellite imagery. For HLS, a fixed number of neighbors ($K = 1$) and the Euclidean distance metric were used. To further improve model performance and spatial consistency, an active learning strategy was adopted to iteratively refine the training set by targeting misclassified samples. Additionally, a systematic sampling approach, based on fixed intervals, was incorporated to reduce random noise and promote coherence across neighboring pixels. The implementation is described in greater detail in the previously referenced study [16]. For Sentinel-2, K was set to 3 with the same distance metric, while for SPOT-6, hyperparameter optimization was performed, with the best results obtained using K set to 14 and the standardized Euclidean distance metric. In all cases, input features were standardized prior to training. The data were randomly divided into 60% for training, 20% for validation, and 20% for testing, with class distributions preserved. Active learning and systematic sampling were also explored for the Sentinel-2 and SPOT-6 datasets; however, they did not lead to meaningful improvements in classification performance. Given the limited effectiveness observed, these techniques were not fully incorporated into the final workflows for these datasets. Separate models were trained for each dataset using the corresponding feature sets described in Section 2.1.

3. Results, Comparison, and Discussion

The classification outputs generated using the KNN model are presented for the HLS, Sentinel-2, and SPOT-6 datasets. For visualization purposes, four representative examples from each dataset were selected. These examples are presented with three columns: the original satellite image, the predicted fuel type map, and the corresponding LANDFIRE ground truth. In the HLS set (Figure 1), predictions appear spatially consistent and in close visual agreement with the reference masks. The Sentinel-2 examples (Figure 2) display moderate spatial alignment with the ground truth. While pixel-level agreement is not always precise, the general structure and distribution of dominant fuel types are largely captured. The SPOT-6 examples (Figure 3) demonstrate a general correspondence between predicted patterns and the underlying satellite imagery. While the spatial layout of major features is reflected in the predictions, notable discrepancies exist when compared to the LANDFIRE ground truth. These differences highlight the coarseness of the reference labels relative to the high-resolution imagery. In several cases, the predicted maps appear visually plausible yet deviate from the blocky, generalized structure of the ground truth, suggesting a misalignment between fine-scale spectral patterns and the resolution of the label source.

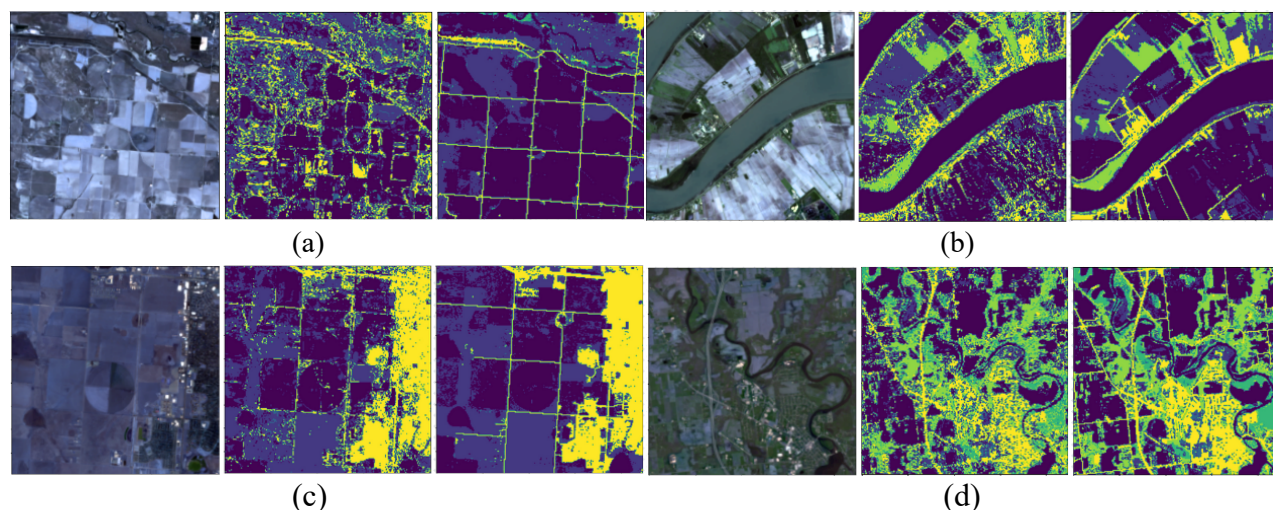


Figure 1. Fuel type classification results for HLS imagery (a–d). Each example includes the original satellite image (left), KNN-prediction (center), and LANDFIRE ground truth (right).

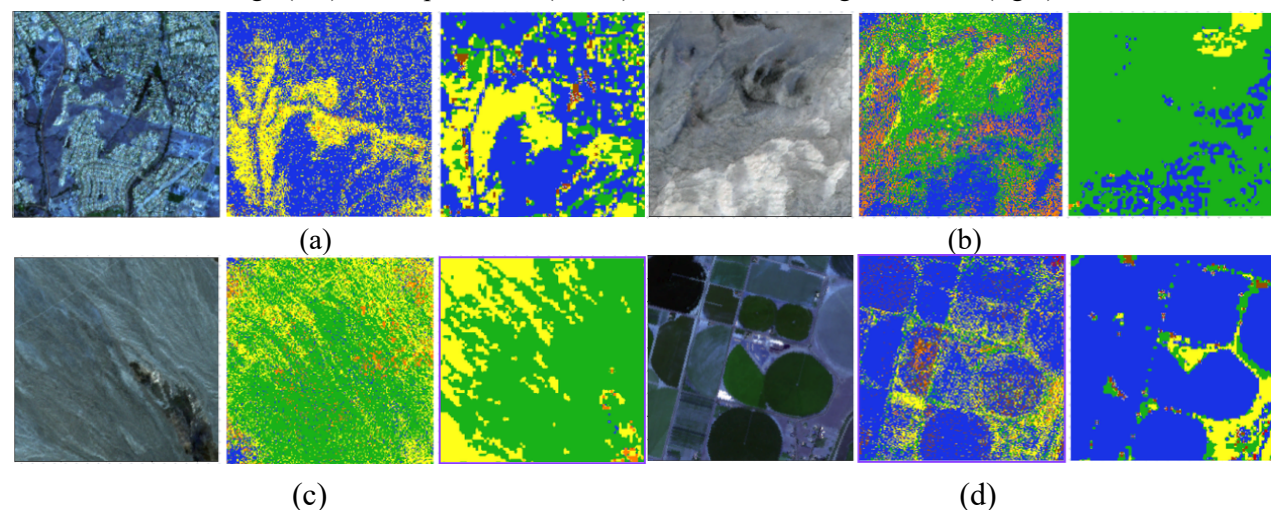


Figure 2. Fuel type classification results for Sentinel2 imagery (a–d). Each example includes the original satellite image (left), KNN-prediction (center), and LANDFIRE ground truth (right).

To complement the qualitative results shown earlier, confusion matrices for each dataset are presented in Figure 4. The KNN classifier achieved an average validation accuracy of 97% for the HLS dataset, 80% for Sentinel-2, and 63% for SPOT-6. These accuracy values provide a general sense of performance but do not fully explain the visual differences observed in the predicted maps. Although these metrics reflect agreement at the pixel level, they do not account for spatial coherence or contextual correctness. The KNN model is trained and evaluated on individual pixels based solely on their feature values and class labels. This approach treats each pixel in isolation, without considering its spatial relationship to neighboring pixels. As a result, even high accuracy may correspond to predictions that differ slightly from expected landscape patterns, particularly in

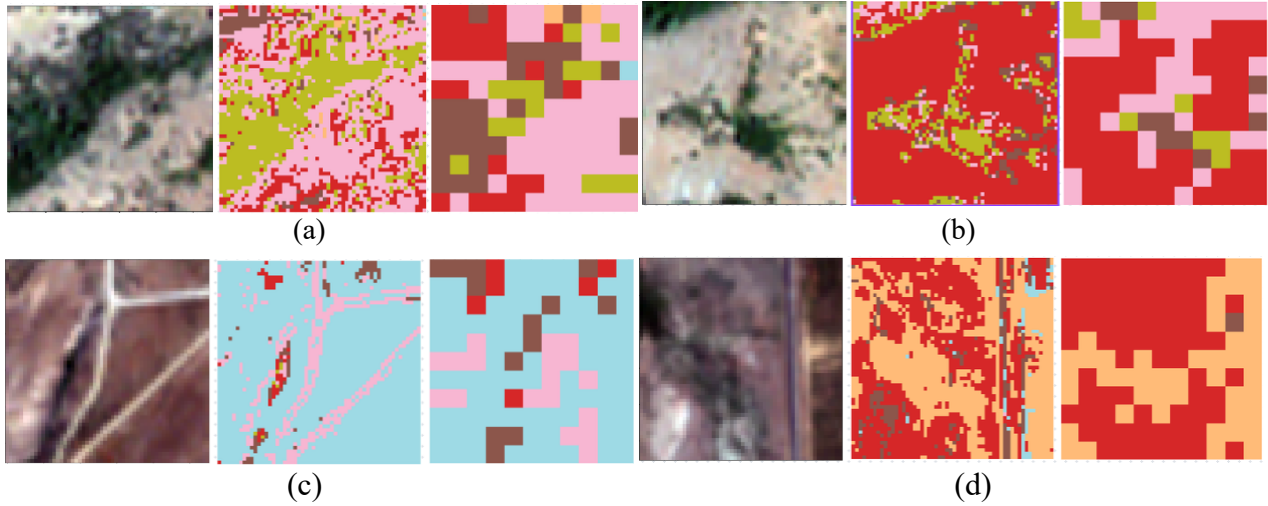


Figure 3. Fuel type classification results for Spot-6 imagery (a–d). Each example includes the original satellite image (left), KNN-prediction (center), and LANDFIRE ground truth (right).

heterogeneous or transitional areas. This highlights the limitation of relying solely on pixel-wise accuracy for interpreting map-level classification results.

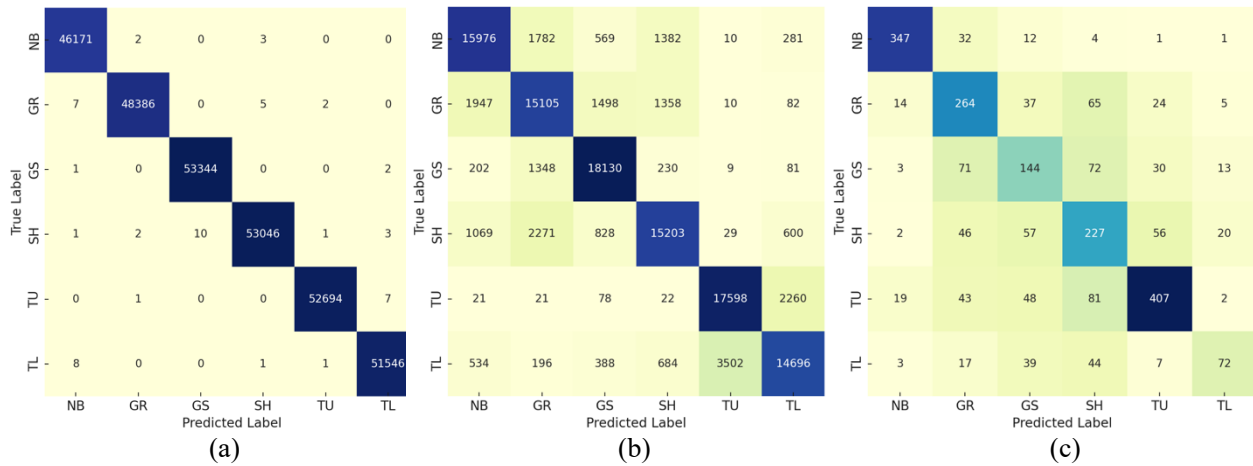


Figure 4. Confusion matrices for fuel type classification using the KNN model across (a) HLS, (b) Sentinel-2, and (c) SPOT-6 datasets.

At first glance, the lower performance of the higher-resolution Sentinel-2 and SPOT-6 datasets may seem counterintuitive, as finer resolution is generally expected to enhance classification accuracy. However, this assumption holds only when ground truth data is both accurate and spatially and temporally well-aligned. In this study, labels were derived from the LANDFIRE data distribution site, which, while widely used, contains inherent noise and generalizations. Additionally, LANDFIRE is a static dataset updated infrequently and may not reflect recent changes in vegetation or land cover. As the satellite imagery used in this study was captured at different times, potential shifts in fuel types between the LANDFIRE reference date and the image acquisition date could introduce further misalignments, compounding the challenges of achieving accurate classification at higher resolutions. At the HLS scale, such misalignment impacts only a single 30×30 m pixel, but at higher resolutions, its effect is magnified. One noisy label can distort 9 pixels in Sentinel-2 (10×10 m) and 25 pixels in SPOT-6 (6×6 m). This amplification, combined with limited labeled data, significantly reduces model performance in high-resolution settings. This discrepancy is clearly illustrated in Figures 2 and 3, where the predicted fuel maps derived from Sentinel-2 and SPOT-6 imagery display realistic and coherent spatial patterns that closely align with the visual characteristics of the original satellite imagery. In these cases, classification accuracy, defined as the ratio of correctly labeled pixels to total pixels, becomes a conceptual metric, reflecting alignment with potentially flawed labels rather than true land cover representation.

Building on these observations, key conclusions are drawn regarding the interplay between image resolution, label quality, and classification performance. In particular, resolution alone does not guarantee better classification outcomes. Instead, what matters is the overall compatibility and quality of both input imagery and ground truth labels. High-resolution data has the potential to capture fine-grained spatial patterns, but if paired with noisy, coarse, or outdated labels, it may introduce greater uncertainty into the training process. Effective classification requires not just detailed imagery, but also equally precise and well-aligned annotations. This limitation becomes especially critical in high-risk or sensitive regions, such as areas surrounding nuclear facilities or critical infrastructure, where precise fuel mapping is essential for risk mitigation. In such cases, relying on coarse, outdated datasets like LANDFIRE can be problematic. As observed in the SPOT-6 results, the fine spatial detail of the imagery was often at odds with the generalized structure of the LANDFIRE labels, leading to visually and numerically inconsistent outcomes. Without high-quality, resolution-compatible ground truth, the full potential of high-resolution imagery cannot be realized.

Additionally, part of the observed performance difference across datasets may be attributed to the volume and balance of available training data. While substantial pixel counts were used for HLS and Sentinel-2, the SPOT-6 dataset included significantly fewer samples, primarily due to the high cost of acquiring high-resolution commercial imagery. This limitation was further compounded by the uneven distribution of vegetation classes across geographically distinct image sets. To maintain class balance during training, the number of usable pixels per class was reduced, limiting the

effective sample size. Although KNN does not require large datasets to function, the reduced data diversity and spatial coverage likely contributed to higher misclassification rates, particularly for minority classes, as reflected in the SPOT-6 confusion matrix. These patterns reinforce the importance of spatial representativeness and sufficient, well-distributed samples when training pixel-based classifiers in heterogeneous landscapes.

Together, these results demonstrate that high-resolution classification is not solely a function of image resolution or algorithmic sophistication. Rather, it requires a holistic integration of high-quality imagery, reliable and resolution-compatible labels, and carefully designed sampling strategies. While KNN proved to be a robust and interpretable model under noisy conditions, its performance and the interpretability of its outputs ultimately depend on the integrity of the inputs and ground truth data. These observations further suggest that satellite imagery at different spatial resolutions may be better suited to different applications. High-resolution data such as SPOT may provide greater value in localized or site-specific analyses, particularly when reliable, fine-scale ground truth is available. In contrast, coarser-resolution products like HLS may be more appropriate for regional-scale classification tasks when supported by spatially compatible reference data. These findings highlight the importance of aligning model selection and data resolution with the intended use case and scale of analysis.

4. Conclusion

This study investigated the potential of utilizing satellite imagery for dynamic fuel mapping, focusing on how varying levels of image detail and label compatibility impact classification accuracy, spatial coherence, and practical usability of fuel mapping. For this purpose, a KNN model was applied to three satellite datasets, HLS, Sentinel-2, and SPOT-6, each offering distinct spatial resolutions. HLS showed the highest validation accuracy and spatial consistency among the three, despite having the coarsest resolution. In contrast, Sentinel-2 and SPOT-6, while offering higher spatial resolution, did not yield better classification accuracy due to increased misalignment between the imagery and the ground truth labels.

Key limitations of this study include the reliance on static LANDFIRE labels as ground truth, whose coarser spatial resolution is not well-matched to the finer resolutions of the Sentinel-2 and SPOT imagery. This mismatch, combined with the inherent noise in the LANDFIRE product, contributes to spatial misalignment and reduced classification reliability when applied to high-resolution inputs. The lack of temporal specificity in LANDFIRE, which reflects generalized vegetation conditions over extended periods, introduces additional uncertainty when compared with satellite imagery acquired at known and discrete time points. Although there were certain limitations, the combination of the KNN model and satellite imagery demonstrated promising potential for application in dynamic fuel mapping, suggesting that with further refinement and validation, this approach could contribute to more accurate and timely assessments of fuel conditions.

Future work should explore ways to enhance label quality, integrate alternative sources of ground truth, or adopt hybrid approaches that combine spatial modeling with pixel-level learning to better capture contextual patterns and improve classification coherence in complex fuel environments.

Acknowledgments

This study has been supported by Google through their Research Scholar Program. This material is also based upon work supported by the National Science Foundation under Grant No. 2237380. The authors sincerely appreciate their supports. Any opinions, findings, and conclusions or recommendations expressed in this material are those of the authors and do not necessarily reflect the views of Google and the National Science Foundation.

References

- [1] S. Mansoor *et al.*, “Elevation in wildfire frequencies with respect to the climate change,” *J. Environ. Manage.*, vol. 301, p. 113769, Jan. 2022, doi: 10.1016/j.jenvman.2021.113769.
- [2] E. A. Kukavskaya, L. V. Buryak, E. G. Shvetsov, S. G. Conard, and O. P. Kalenskaya, “The impact of increasing fire frequency on forest transformations in southern Siberia,” *For. Ecol. Manag.*, vol. 382, pp. 225–235, Dec. 2016, doi: 10.1016/j.foreco.2016.10.015.
- [3] J. D. Coop *et al.*, “Wildfire-Driven Forest Conversion in Western North American Landscapes,” *BioScience*, vol. 70, no. 8, pp. 659–673, Aug. 2020, doi: 10.1093/biosci/biaa061.
- [4] R. J. Whelan, “The Ecology of Fire - Developments since 1995 and Outstanding Questions,” *Proc. R. Soc. Qld.*, vol. 115, pp. 59–68, Apr. 2009, doi: 10.5962/p.357727.
- [5] D. Vakalis, H. Sarimveis, C. Kiranoudis, A. Alexandridis, and G. Bafas, “A GIS based operational system for wildland fire crisis management I. Mathematical modelling and simulation,” *Appl. Math. Model.*, vol. 28, no. 4, pp. 389–410, Apr. 2004, doi: 10.1016/j.apm.2003.10.005.
- [6] M. G. Rollins, “LANDFIRE: a nationally consistent vegetation, wildland fire, and fuel assessment,” *Int. J. Wildland Fire*, vol. 18, no. 3, p. 235, 2009, doi: 10.1071/WF08088.
- [7] A. L. DeCastro, T. W. Juliano, B. Kosović, H. Ebrahimian, and J. K. Balch, “A Computationally Efficient Method for Updating Fuel Inputs for Wildfire Behavior Models Using Sentinel Imagery and Random Forest Classification,” *Remote Sens.*, vol. 14, no. 6, p. 1447, Mar. 2022, doi: 10.3390/rs14061447.
- [8] P. Barmpoutis, P. Papaioannou, K. Dimitropoulos, and N. Grammalidis, “A Review on Early Forest Fire Detection Systems Using Optical Remote Sensing,” *Sensors*, vol. 20, no. 22, p. 6442, Nov. 2020, doi: 10.3390/s20226442.
- [9] J. Wallace, G. Behn, and S. Furby, “Vegetation condition assessment and monitoring from sequences of satellite imagery,” *Ecol. Manag. Restor.*, vol. 7, no. s1, Jun. 2006, doi: 10.1111/j.1442-8903.2006.00289.x.
- [10] S. Talukdar *et al.*, “Land-Use Land-Cover Classification by Machine Learning Classifiers for Satellite Observations—A Review,” *Remote Sens.*, vol. 12, no. 7, p. 1135, Apr. 2020, doi: 10.3390/rs12071135.
- [11] P. Jain, S. C. P. Coogan, S. G. Subramanian, M. Crowley, S. Taylor, and M. D. Flannigan, “A review of machine learning applications in wildfire science and management,” *Environ. Rev.*, vol. 28, no. 4, pp. 478–505, Dec. 2020, doi: 10.1139/er-2020-0019.

- [12] A. D. P. Pacheco, J. A. D. S. Junior, A. M. Ruiz-Armenteros, and R. F. F. Henriques, "Assessment of k-Nearest Neighbor and Random Forest Classifiers for Mapping Forest Fire Areas in Central Portugal Using Landsat-8, Sentinel-2, and Terra Imagery," *Remote Sens.*, vol. 13, no. 7, p. 1345, Apr. 2021, doi: 10.3390/rs13071345.
- [13] LP DAAC, "Harmonized Landsat and Sentinel-2 (HLS) Overview." [Online]. Available: <https://lpdaac.usgs.gov/data/get-started-data/collection-overview/missions/harmonized-landsat-sentinel-2-hls-overview/>.
- [14] European Space Agency (ESA), "Copernicus Sentinel-2 — Mission Overview." [Online]. Available: https://www.esa.int/Applications/Observing_the_Earth/Copernicus/Sentinel-2
- [15] European Space Agency (ESA), "SPOT 6/7 - Earth Online," ESA Earth Observation Gateway. [Online]. Available: <https://earth.esa.int/eogateway/missions/spot-6>
- [16] N. Rashidi and J. Y. Lee, "Dynamic Fuel Mapping Using Satellite Imagery and AI Techniques".